THE PUBLISHING HOUSE
OF THE ROMANIAN ACADEMY

PROCEEDINGS OF THE ROMANIAN ACADEMY, Series A,
Special Issue/2018, pp. 279–284

CONSTRUCTAL DESIGN OF A NON-INVASIVE TEMPERATURE BASED MASS FLOW RATE SENSOR FOR ALGAE PHOTOBIOREACTORS

Kassiana RIBEIRO[1,2], Juan C. ORDONEZ[1,2], José V.C. VARGAS[1,2], and André B. MARIANO[2]

[1] Florida State University, Department of Mechanical Engineering, Energy and Sustainability Center and Center for Advanced Power Systems, Tallahassee, Florida, 32310, USA
[2] Federal University of Paraná, Sustainable Energy Research and Development Center (NPDEAS), Curitiba, Brazil
Corresponding author: Juan ORDONEZ, E-mail: jordonez@fsu.edu

Abstract. Microalgae are among the best-established life forms on earth and have been identified as likely sources of biofuels [1]. Controlled cultivation of microalgae in photobioreactors, PBR, requires the ability of monitoring and sensing key process variables (e.g., CO_2 levels, mass flow rates, irradiance). The current work is aimed at improving the use of compact transparent pipes photobioreactors for continuous microalgae growth through the development of a non-invasive mass flow rate sensor that can be used as an alternative to more expensive commercially available ones. The paper presents a Volume Element Model (VEM) for a temperature based mass flow rate sensor, that combines principles of thermodynamics, heat transfer, and fluid mechanics and discretizes the system in space, resulting in a system of ordinary differential equations with respect to time that allows for the exploration of design parameters following a constructal approach. A sensor total volume constraint is identified, and the sensor shape is optimized for minimum entropy generation, which results in maximum temperature difference measurements, which are proportional to pipe mass flow rate, thus increasing sensitivity and reducing cost. Sharp maxima were obtained for the sensor flow temperature difference, depicting a 97% variation for ΔT in the range $0.01 \le R_1/R_4 \le 0.3$, for $\dot{Q}_{gen} = 10$ W and $\dot{m} = 0.1$ kg s^{-1}. The results illustrate how following a constructal design approach, it is possible to tune the system resistances to heat transfer in order to achieve a functional design.

***Key words*:** Second Law of Thermodynamics, Constructal Design, Flow sensor, Shape optimization.

1. INTRODUCTION

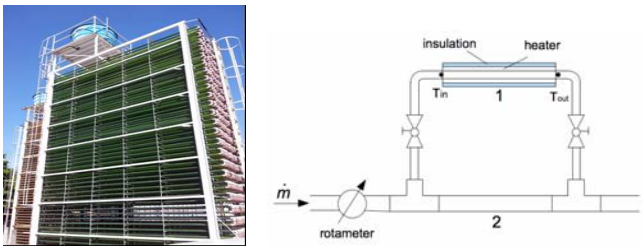

Fig. 1 – Left: compact tubular photobioreactor at Federal University of Parana, Curitiba, Brazil, and right: branching used for the proposed mass flow rate sensor.

Batch cultivation is a typical form of chemical reactors operation that is used to grow microalgae in large scale compact tubular photobioreactors [1–3], such as the type shown in Fig. 1. An alternative to this mode of operation is a continuous cultivation, in which the photobioreactor continues to operate with the highest cell concentration for a longer time. In this system dilution and biomass harvesting are done in a continuous way, therefore integrated mass flow and concentration sensors are needed to properly monitor the process. An extensive review of microalgae growth kinetics mathematical models was recently conducted [4]. The study pointed out the need for the development of non-invasive sensors [5–7] in order to avoid cultivation disturbances, and therefore imprecisions in the determination of required model constants. The present study establishes two objectives to address this need: i) to propose a new non-invasive thermal mass flow rate sensor design, and ii) to introduce a dynamic mathematical model for the proposed sensor in order to produce a system constructal design [8] based on the entropy generation minimization method. To achieve that, the model is based on the physical laws, i.e., mass and energy conservation principles, so that reliability is assured for possible future use in design, control and optimization of photobioreactors or any other system.

2. MATHEMATICAL MODEL

In order to reduce the flow rate going through the sensor, the configuration illustrated in Fig. 1 (right) is proposed. Accordingly, the main photobioreactor pipe is branched into a section of reduced diameter to which the heating element is attached, the rotameter is used only to calibrate the sensor. With this configuration, the relationship between the flow rate in the main pipe and the mass flow rate going through the heater derivation pipe is dictated by the difference in flow resistance in branches 1 and 2, and is obtained from the solution of the simple flow network. Using mass conservation, $\dot{m} = \dot{m}_1 + \dot{m}_2$, where $\dot{m}$, $\dot{m}_1$ and $\dot{m}_2$ are the mass flow rates in the main pipe, branch 1, and branch 2, respectively, kg s^{-1}, and ensuring that the pressure drop (due to major and minor losses) along branches 1 and 2 must be equal, therefore

$$\frac{K_1}{2} + 2f_1 \frac{L_1}{D_1}\rho,$$

$$K_1 = K_{T(bf),1} + K_{sc} + K_{val,1} + K_{90,1} + K_{90,2} + K_{val,2} + K_{se} + K_{T(bf),2}, \tag{1}$$

$$K_2 = K_{T(tf),1} + K_{T(tf),2},$$

where ρ is the fluid density; L_1 and L_2 the total length of branches 1 and 2 ducts, respectively; D_1 and D_2 the hydraulic diameters in branches 1 and 2 respectively; K_1 the sum of the minor loss coefficients in branch 1 due to the two tees (branching flow), a sudden contraction, two valves, two 90-degree turns and a sudden expansion, as it is shown in Table 1.

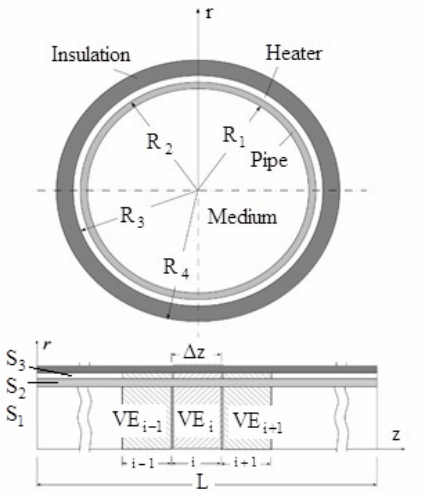

Fig. 2 – Top: schematic representation of the sensor cross sectional, and bottom: volume elements and systems within the VE.

K_2 is the sum of minor loss coefficients in branch 2: two tees (through flow). In eq. (1) f_1 and f_2 are the Fanning friction factors, which are obtained [9] as $f = 16/\mathrm{Re}_{D_k}$ for $\mathrm{Re}_{D_k} < 2{,}300$ and $f = 0.079\,\mathrm{Re}_{D_k}^{-1/4}$ for $\mathrm{Re}_{D_k} > 2{,}300$ $(k = 1, 2)$, where $\mathrm{Re}_{D_k} = \dfrac{V_k D_k}{\nu}$ is the Reynolds number, $V_k = \dfrac{\dot{m}_k}{\rho A_{c,k}}$ is the fluid velocity [ms^{-1}]; ν – the fluid kinematic viscosity branch k pipe, and $A_{c,k}$ – the cross sectional area of the branch k pipe [m^2].

To calculate the sensor temperature differential it is necessary to compute the temperature distribution in the sensor branch (branch 1). For that, a Volume Element Model (VEM) [11, 12] is developed. The solution domain is discretized in small Volume Elements (VE) in the z direction as illustrated in Fig. 2. Each VE is comprised by 3 systems: S_1 – algae/water (medium); S_2 – pipe wall, and S_3 – heater. The first law of thermodynamics is applied to each system in the VE. Constitutive and heat transfer equations are used to evaluate the physical properties and heat transfer rates between the VE, respectively. A similar approach has been employed previously in the modelling and optimization of energy systems engineering (*e.g.* [11–14]).

2.1. System 1 (algae/water medium)

The first law of thermodynamics applied to the S_1 in VE i shown in Fig. 2 states that:

$$m_1^i c_1 \frac{\mathrm{d}T_1^i}{\mathrm{d}t} = \dot{Q}_{12}^i + \dot{Q}_{cv}^i; \quad \dot{Q}_{cv}^i = \dot{m}_1\, c_1 \left(T_1^{i-1} - T_1^i\right); \quad \dot{Q}_{12}^i = (UA)_{12}^i \left(T_2^i - T_1^i\right), \tag{3}$$

in which superscript i refers to VE i, for $1 \le i \le n$, with n being the total number of VE that discretizes the

sensor as shown in Fig. 2 (bottom); $\dot{Q}$[W] is the heat transfer rate; $m_j^i = (\rho V)_j^i$ [kg] – the mass of the material (medium, pipe, or heater) within S_j (j = 1, 2 or 3, as shown in Fig. 2) in VE i; ρ [kg m^{-3}] – the density; V [m^3] – the volume; T [K] – the temperature; t [s] – the time, and c [J kg^{-1} K^{-1}] – the specific heat.

Table 1

Loss coefficients expressions and values used in the simulation [10]

Component	Loss coefficient
Sudden expansion; Sudden contraction; Tee (branching flow)	$K_{se} = \left\{1 - \left(\frac{D_2}{D_1}\right)^2\right\}^2$; $K_{sc} = \frac{0.5\left\{1 - \left(\frac{D_2}{D_1}\right)^2\right\}}{\left(\frac{D_2}{D_1}\right)^4}$; $K_{T(bf),1} = K_{T(bf),2} = 1.62$
Tee (through flow); Ball valve; 90^o elbow	$K_{T(tf),1} = K_{T(tf),2} = 0.54$; $K_{val,1} = K_{val,2} = 9.2$; $K_{90,1} = K_{90,2} = 0.8$

The thermal conductance and the Nusselt number correlations for both laminar and transient regimes [9, 10] are calculated by

$$(\mathrm{UA})_{12}^{\mathrm{i}} = \left\{ \frac{\ln\left(\frac{R_1 + R_2}{2R_1}\right)}{2\pi k_2 \Delta z^i} + \frac{1}{2\pi R_1 \Delta z^i h} \right\}^{-1}, \begin{cases} \mathrm{Re}_{D_1} < 2{,}300 : \mathrm{Nu}_{D_1} = 4.36 \text{ (uniform heat flux)} \\ \mathrm{Re}_{D_1} > 2{,}300 : \mathrm{Nu}_{D_1} = \dfrac{(f_1/2)(\mathrm{Re}_{D_1} - 1000)\,\mathrm{Pr}}{1 + 12.7(f_1/2)^{1/2}(\mathrm{Pr}^{2/3} - 1)} \end{cases}, \tag{4}$$

where U is the overall heat transfer coefficient; A [m^2] is the heat transfer area; R [m] is the system radius as shown in Fig. 2; k is [W m^{-1} K^{-1}] the thermal conductivity; Δz^i [m] is the VE i length; $\mathrm{Re}_{D_1} > 2{,}300$ (turbulent regime), the Gnielinski correlation is valid for $0.5 \le \mathrm{Pr} \le 2{,}000$, and $\mathrm{Re}_{D_1} \le 5 \times 10^6$, and Pr is the fluid Prandtl number. For the aqueous microalgae medium in this work, $\mathrm{Pr} \cong 7$. The convective heat transfer coefficient, h, is then calculated via $h = k_1\,\mathrm{Nu}_{D_1}/D_1$.

2.2. System 2 (pipe)

$$m_2^i c_2 \frac{\mathrm{d}T_2^i}{\mathrm{d}t} = -\dot{Q}_{12}^i + \dot{Q}_{23}^i + \dot{Q}_{2,c,in}^i - \dot{Q}_{2,c,out}^i; \quad \begin{cases} \dot{Q}_{2,c,in}^i = -\dfrac{k_2 A_{c,2}(T_2^i - T_2^{i\text{-}1})}{(\Delta z^i + \Delta z^{i-1})/2}, \\ \dot{Q}_{2,c,out}^i = -\dfrac{k_2 A_{c,2}(T_2^i - T_2^{i+1})}{(\Delta z^i + \Delta z^{i+1})/2}. \end{cases} \tag{5}$$

Equation (5) relies upon the first law of thermodynamics applied S_2, so that the second system represents the pipe walls, in which m_2^i is the medium mass within S_2 in VE i [kg]; the subscripts c, in and out indicate conduction heat transfer, inlet and outlet, respectively. Equation (5) also accounts for the convective heat transfer rate absorbed by the algae stream, $\dot{Q}_{12}^i$, and the conduction heat transfer rate through the pipe walls between VE i and its two neighbors, $\dot{Q}_{2,c,in}^i$ and $\dot{Q}_{2,c,out}^i$. Note that when $i = 1$ and n, $\dot{Q}_{2,c,in}^1 = 0$ and $\dot{Q}_{2,c,out}^n = 0$, respectively, assuming the negligible heat leak rate to the ambient in the axial direction at the sensor left and right sides. The conduction heat transfer rate between S_2 and S_3 is calculated by $\dot{Q}_{23}^i = (\mathrm{UA})_{23}^i (T_2^i - T_1^i)$ with $(\mathrm{UA})_{23}^{\mathrm{i}} = \{\ln(2R_2/(R_1+R_2)) / (2\pi k_2 \Delta z^i) + \ln((R_2 + R_3)/(2R_2))/(2\pi k_3 \Delta z^i)\}^{-1}$.

2.2.3. System 3 (heater)

For the heater system, the first law requires that:

$$m_3^i c_3 \frac{\mathrm{d}T_3^i}{\mathrm{d}t} = -\dot{Q}_{23}^i + \dot{Q}_{gen}^i + \dot{Q}_{3,c,in}^i - \dot{Q}_{3,c,out}^i - \dot{Q}_{\infty}^i, , \tag{8}$$

where the conduction heat transfer rates $\dot{Q}_{3,c,in}^i$ and $\dot{Q}_{3,c,out}^i$ for the heater are calculated similarly to what was done for system 2; $\dot{Q}_{gen}^i$ is the heat rate generated by the heater, so that taking h_∞ [W m^{-2} K^{-1}] as the convection heat transfer coefficient between the insulation external surface and the environment; $\dot{Q}_{\infty}^i = (\mathrm{UA})_{3\infty}^{\mathrm{i}}(T_3^i - T_\infty^i)$ is the heat leak rate through the insulation to the ambient; $(\mathrm{UA})_{3\infty}^{\mathrm{i}}$ = {ln(R_4/R_3)·(2πk_{ins}Δz^i)$^{-1}$+ +ln(2R_3/(R_2+R_3))·(2πk$_3$Δz$^{\mathrm{i}}$)$^{-1}$ +(2πR_4Δz^{i} h_∞)$^{-1}$}$^{-1}$; h_∞ [W m^{-2} K^{-1}] is the convection heat transfer coefficient between the insulation external surface and the environment, and subscripts *ins* and 3∞ for the insulation, and the interaction between system 3 and the ambient, respectively.

2.3. Physical properties

The thermo-physical properties of the algae/water were evaluated at atmospheric pressure (101,325 Pa) and 20°C, the dimensions and additional physical properties used in a base case simulation are (c_1, c_2, c_3) = = (4180, 385, 450) J kg^{-1} K^{-1}; (k_1, k_2, k_3, k_{ins}) = (0.591, 401, 11.3, 1) W m^{-1} K^{-1}; (D_2, L_1, L_2) = (0.0508, 0.3, 1) m; (R_1, R_2, R_3, R_4) = (0.0067, 0.00795, 0.0125, 0.0245) m; h_∞ = 5 W m^{-2} K^{-1}; $\dot{m}$ = 0.1 kg s^{-1}, $\dot{Q}_{gen}$ = 10 W, $T_{in} = T_\infty$ = 293.15 K, (ρ = ρ$_1$, ρ$_2$, ρ$_3$) = (1,000, 8,933, 8,400) kg m^{-3}, and the initial conditions are $\vec{T}_{1,0} = \vec{T}_{2,0} = \vec{T}_{3,0} = 293.15$ K.

3. THE CONSTRUCTAL DESIGN

One objective function is selected to evaluate the sensor system total entropy generation rate, $\dot{S}_{gen}$, which should be minimized. Considering a control volume involving the sensor shown in Fig. 2, from the inlet to the outlet and limited by the insulation external surface, for an incompressible liquid, the second law of thermodynamics states that:

$$\dot{S}_{gen} = -\sum_{i=1}^{n} \frac{\dot{Q}_\infty^i}{T_{ins}^i} + \dot{m}_1 c_1 \ln\frac{T_{out}}{T_{in}} \geq 0; \quad T_{ins}^i = T_3^i + \frac{\dot{Q}_\infty^i}{(\mathrm{UA})_{3\infty}^{\mathrm{i}}}; \quad (\mathrm{UA})_{3ins}^{\mathrm{i}} = \left\{ \frac{\ln\left(\frac{R_4}{R_3}\right)}{2\pi k_{ins}\Delta z^i} + \frac{\ln\left(\frac{2R_3}{R_2+R_3}\right)}{2\pi k_3 \Delta z^i} \right\}^{-1}, \tag{10}$$

where $T_{in} = T_1^1$, $T_{out} = T_1^n$, and T_{ins}^i is the temperature at the insulation external surface in VE 1; the subscript 3*ins* refers to the thermal conductance between system 3 and the insulation external surface. The second objective function is the total sensor fluid temperature difference, which is evaluated with $\Delta T = T_1^n - T_1^1$. Since the sensor hardware, i.e., pipe, heater and insulation, shown in branch 1 of Fig.1, are commodities in short supply, it makes sense to recognize the total sensor volume as a physical constraint for the optimization problem. For a fixed length L_1, and circular cross section, the sensor total volume constraint is represented by a fixed outer radius, R_4, as it is defined in Fig. 5, so that $R_1 + t_p + t_h + t_{ins} = R_4$.

There are 3 geometric parameters to optimize, and the fourth results from them. Therefore, assuming fixed pipe and heater thicknesses, t_p = 0.00125 m and t_h = 0.00455 m, as additional constraints, the optimization problem is reduced to find the optimal pipe inner radius, $R_{1,opt}$, that maximizes ΔT and minimizes $\dot{S}_{gen}$, and the optimal insulation thickness, $t_{ins,opt}$, that results from $R_{1,opt}$.

4. RESULTS AND DISCUSSION

Figure 5 illustrates the system temperature transient response toward steady state in the last volume element. The time to reach steady state is approximately 1 hour. The sensor temperature distribution at steady state is shown in Fig. 6. Both figures are for for $\dot{Q}_{gen} = 10$ W and $\dot{m} = 0.1$ kgs^{-1}.

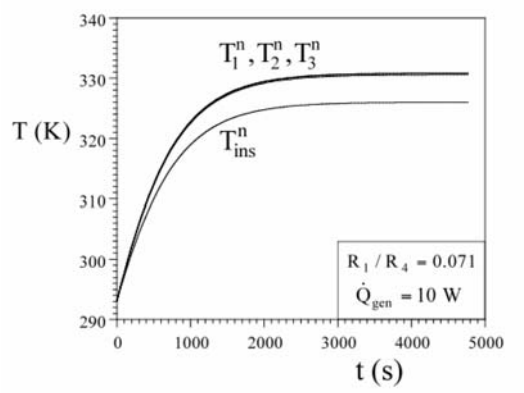

Fig. 5 – The temperature transient evolution in VE *n* (z = 0.2925m).

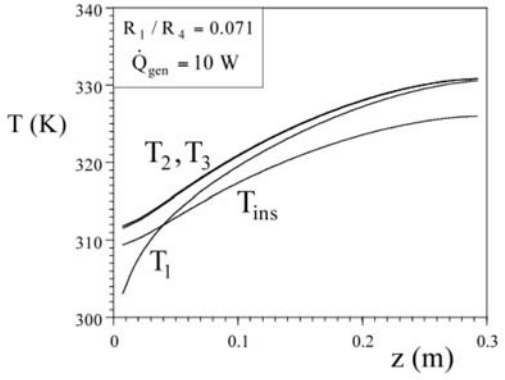

Fig. 6 – The steady state temperature distribution.

The pipe and heater systems are almost in thermal equilibrium, the fluid at a lower temperature, and the insulation external surface at a significantly lower temperature as expected. All temperatures increase as z increases as the fluid accumulates heat that is driven from the heater. This effect creates the temperature differential that is proportional to the pipe mass flow rate, i.e., the ultimate sensor measurement. Note that, in spite of the low heat input rate, the sensor design herein proposed is capable of producing an easily measurable ΔT. Next, the study proceeds in pursuit of the sensor constructal design. For that, the optimization procedure described in section 3 is conducted. The existence of an optimal pipe inner radius to outer insulation radius, $(R_1 / R_4)_{opt}$, is physically explained by analyzing two extremes: i) when $R_1 / R_4 \to 0$, $\dot{m}_1 \to 0$, and the heat generated by the heater is uniformly distributed in the sensor by conduction, so that $\Delta T \to 0$, and ii) when R_1 / R_4 is large, $\dot{m}_1$ increases so that for fixed $\dot{Q}_{\text{gen}}$, $\Delta T \to 0$ as well. Hence, there must be an intermediate and optimal value for R_1 / R_4 so that ΔT is maximum. Such system tradeoffs apply similarly to the system total entropy generation rate. Fig. 7 shows the optimization results. Even for such low heater power input, a sharp maximum is found with respect to R_1 / R_4, depicting $\Delta T_{\max} = 27.5$ K for $(R_1 / R_4)_{opt} = 0.071$. Regarding the entropy generation rate, it is found that $(R_1 / R_4)_{opt} = 0.1$ with $\dot{S}_{gen,\min} = 0.022$ W K^{-1} and $\Delta T = 18.2$ K whereas for $R_1 / R_4 = 0.071$, $\dot{S}_{gen} = 0.0245$ W K^{-1} and $\Delta T_{\max} = 27.5$ K, i.e., approximately a 10% and 50% increase in $\dot{S}_{gen}$ and ΔT, respectively. Fig. 8 demonstrates the robustness of the optima with respect to the variation of $\dot{Q}_{gen}$.

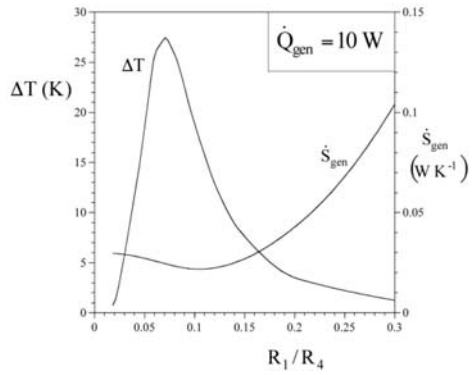

Fig. 7 – The maximization of ΔT and minimization of $\dot{S}_{gen}$ for $\dot{Q}_{gen} = 10$ W and $\dot{m} = 0.1$ kg s^{-1}.

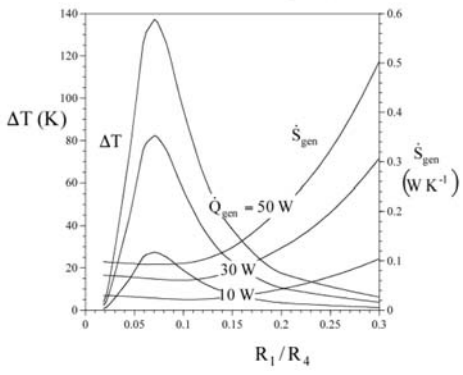

Fig. 8 – The variation of $\dot{Q}_{gen}$ on the maximization of ΔT and minimization of $\dot{S}_{gen}$ for $\dot{m} = 0.1$ kg s^{-1}.

5. CONCLUSIONS

A novel constant current noninvasive thermal mass flow rate sensor has been proposed. The temperature measurement based sensor is placed in a derivation branch of the main pipe, where only a small fraction of the flow is routed. The temperature difference across the sensor is later correlated to the total mass flow rate. A mathematical model was also developed for sizing and thermodynamically optimizing the sensor for maximum flow temperature difference and minimum entropy generation, therefore finding the sensor constructal design. Sharp maxima were obtained for the sensor flow temperature difference, depicting a 97% variation for ΔT in the range $0.01 \le R_1 / R_4 \le 0.3$, for $\dot{Q}_{gen} = 10\,\mathrm{W}$ and $\dot{m} = 0.1\,\mathrm{kg\,s^{-1}}$. This aspect stresses the importance of finding the sensor constructal design so that high performance is obtained.

ACKNOWLEDGEMENTS

The authors acknowledge support ONR grant N00014-16-1-2956, CNPq, Brazil, projects 407198/2013-0, 403560/2013-6, 407204/2013-0, and 302938/2015-0; contracts 41-2013/UFPR/PSA, and 111-2014/UFPR/NILKO Tecnologia Ltd.

REFERENCES

1. SATYANARAYANA, K.G., MARIANO, A.B., VARGAS, J.V.C., *A review on microalgae, a versatile source for sustainable energy and materials,* International Journal of Energy Research, **35**, pp. 291–311, 2011.
2. VARGAS, J.V.C., BALMANT, W., STALL, A., MARIANO, A.B., ORDONEZ, J.C., HOVSAPIAN, R., DILAY, E., Patent Number US2012088296-A1 and WO2012050608-A1 – US Patent and Trademark Office, 2012.
3. VARGAS, J.V.C., MARIANO, A.B., CORRÊA, DO., ORDONEZ, J. C., *The microalgae derived hydrogen process in compact photobioreactors*, International Journal of Hydrogen Energy, **39**, pp. 9588–9598, 2014.
4. LEE, E., JALALIZADEH, M., ZHANG, Q., *Growth kinetic models for microalgae cultivation: A review*, Algal Research, **12**, pp. 497–512, 2015.
5. DIGIACOMO, R., *Review of industrial processing flowmeters*, White paper, *ABB Flowmeters*, ABB Measurement Products, 2012.
6. WILSON, J.S., *Sensor Technology Handbook* (Chapter 10), Elsevier, Saint Louis, US, 2004.
7. FINGERSON, L.M., *Thermal anemometry, current state, and future directions*, Rev. Sci. Instrum., **65**, *2*, pp. 285–300, 1994.
8. BEJAN, A., *Shape and Structure, from Engineering to Nature*, Cambridge University Press, 2000.
9. INCROPERA, F.P., DEWITT, D.P., BERGMAN, T.L., LAVINE, A.S., *Fundamentals of Heat and Mass Transfer*, 6th ed., Wiley, 2007.
10. SHAMES, I. H., *Mechanics of Fluids*, London, McGraw-Hill, 2003.
11. VARGAS, J.V.C., STANESCU, G., FLOREA, R., CAMPOS, M.C., *A numerical model to predict the thermal and psychrometric response of electronic packages*, ASME Journal of Electronic Packaging, **123**, *3*, pp. 200–210, 2001.
12. DILAY, E., VARGAS, J.V.C., SOUZA, J.A., ORDONEZ, J.C., YANG, S., MARIANO, A.B., *A volume element model (VEM) for energy systems engineering*, Int. J. Energy Res., **39**, pp. 46–74, 2015.
13. ORDONEZ, J.C., VARGAS, J.V.C., HOVSAPIAN, R., *Modeling and simulation of the thermal and psychrometric transient response of all-electric ships, internal compartments and cabinets*, Simulation, **84**, *8–9*, pp. 427–439, 2008.
14. ORDONEZ, J.C., SOUZA, J.A., SHAH, D.R., VARGAS, J.V.C., HOVSAPIAN, R., *Temperature and pressure drop model for gaseous helium cooled superconducting DC cables*, IEEE Transactions on Applied Superconductivity, **23**, *3*, pp. 5402005, 2013, doi:10.1109/TASC.2013.2241380.